Molecular Dosimetry of N7-Guanine Adducts in Male and Female Mice Exposed to 1,3-Butadiene by Inhalation

John Mitchell Troutman

A thesis submitted to the faculty of the University of North Carolina at Chapel Hill in partial fulfillment of the requirements for the degree of Master of Science in the Curriculum in Toxicology.

Chapel Hill
2011

Approved by:
James A. Swenberg, DVM, PhD
Wanda M Bodnar, PhD
Louise M. Ball, PhD

Abstract

John Mitchell Troutman: Molecular Dosimetry of N7-Guanine Adducts in Male and Female Mice Exposed to 1,3-Butadiene by Inhalation

(Under the direction of Dr. James A. Swenberg)

1,3-Butadiene (BD) is a well-characterized carcinogen that is both an occupational and environmental hazard and an important industrial chemical widely used in the production of rubber and plastic and is also present in automobile exhaust and cigarette smoke. Upon metabolic activation in vivo, it forms three epoxides that can react with nucleophilic sites in biomolecules: 1,2,3,4-diepoxybutane (DEB), 1,2-epoxy-3-butene (EB), and 3,4-epoxy-1,2-butane-diol (EBD). We characterized the molecular dosimetry of N-7 guanine adduct formation by these metabolites of BD in the liver of male and female B6C3F1 mice exposed to varying concentrations of BD. The adducts, racemic and meso forms of N-7-(2,3,4-trihydroxy-3-buten-2-yl)guanine (THB-Gua), N-7-(2-hydroxy-3-buten-1-yl)guanine (HB-Gua I), and N-7-(1-hydroxy-3-buten-2-yl)guanine (HB-Gua II) were similar in male and female B6C3F1 mice at all levels where liver tissue was available for both sexes. Thus, no gender differences in adduct formation were noted. The THB-Gua adducts were the most abundant and exhibited a supralinear dose response.

To my family and all my pets (past and present): to err is human, to forgive feline. In memoriam of my cat named “fish” who will always have a special place in my heart and mind. Lastly, I shall end this dedication with my favorite quote from Rudolf Virchow: “*Between animal and human medicine there is no dividing line—nor should there be. The object is different but the experience obtained constitutes the basis of all medicine.”*

Table of Contents

List of Tables

List of Scheme and Figures

List of Abbreviations

BD – 1,3-butadiene

bis-N7G-BD – 1,4-bis(guan-7-yl)-2,3-butanediol

BD-diol – butane diol

DEB – 1,2,3,4-diepoxybutane

DNA – deoxyribonucleic acid

EB – 3,4-epoxy-1-butene

EBD - 3,4-epoxy-1,2-butanediol

FA – Fanconi anemia

Gua – guanine

HB-Gua I – N-7-(2-hydroxy-3-buten-1-yl)guanine

HB-Gua II – N-7(1-hydroxy-3-buten-2-yl)guanine

HPLC-ESI$^+$-MS/MS – high performance liquid chromatography-electrospray ionization tandem mass spectrometry

LC/ESI$^+$-MS/MS – liquid chromatography-electrospray ionization tandem mass spectrometry

MFs – mutant frequencies

ppm – parts per million

pyr-Val – N,N-(2,3-dihydroxy-1,4-butadiyl)valine

SD – standard deviation

SRM – selected reaction monitoring

THB-G – N7-(2,3,4-trihydroxy-1-yl)guanine

THB-Gua – N7-(2,3,4-trihydroxy-1-yl)guanine

Chapter 1

Introduction

1,3-Butadiene (BD) is a petrochemical widely used in the production of synthetic rubber and plastic *(1)*. It is also an environmental toxin found in automobile exhaust, fossil fuels, and in cigarette smoke *(2;3)*. Recently, BD has been rated the cigarette constituent with the highest cancer risk index *(4)*. BD is classified by the USEPA and IARC as a human carcinogen based on human epidemiologic studies and laboratory animal data *(5;6)*. Human epidemiologic studies have shown an increased incidence of leukemia in workers exposed to BD in synthetic rubber production and an increase in lymphohematopoietic cancers in BD production workers that were not exposure related *(6-10)* . Long term inhalation exposure of mice and rats to BD caused the development of tumors at multiple sites *(11-13)*, with mice developing cancer at exposures 160 times lower than rats and therefore being a much more sensitive species than rats *(6)*. The complexity of BD carcinogenesis has been attributed mainly to species-dependent differences in BD metabolism.

Bioactivation of BD in animal and human tissues to yield reactive epoxides is an important determinant of the mutagenic and carcinogenic effects of BD *(14)*. Upon metabolic activation, BD is first oxidized to 3,4-epoxy-1-butene (EB), which can be further oxidized to 1,2,3,4-diepoxybutane (DEB) or can be metabolized by epoxide hydrolase (EH) to form 1-butene-3,4-diol (Scheme 1), which can be further metabolized to 3,4-epoxy-1,2-

butanediol (EBD) *(15-19)*. The three epoxide metabolites of BD (EB, DEB, and EBD) are reactive electrophiles capable of binding to nucleophilic sites within biomolecules such as

Scheme 1. Metabolism of BD to DNA-Reactive Epoxides

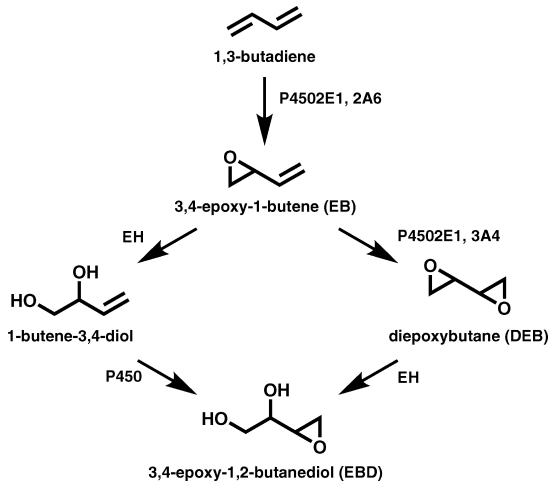

proteins and DNA to form covalent adducts *(20;21)* (Figure 1). Both EB and DEB are direct-acting mutagens, which are believed to play important roles in the mutagenicity/carcinogenicity of BD. However, BD derived metabolites differ in their mutagenic potency up to 200 fold with DEB being the most mutagenic metabolite *(22-27)*. Thus, DEB is considered the most carcinogenic metabolite of BD because of its potent genotoxicity and its ability to form bifunctional DNA adducts such as exocyclic DNA lesions and DNA-DNA cross-links *(24;28-30)* . DEB preferentially alkylates the N-7 position of guanine bases in DNA to form N-7-(2-hydroxy-3,4-epoxybut-1-yl)-guanine (N-7-HEB-dG) adducts *(30;31)*. The epoxide group of N-7-HEB-dG can then be hydrolyzed to N-7-(2,3,4-trihydroxybut-1-yl)-guanine (THB-G) *(28;30)*. The formation of pro-mutagenic DNA adducts define the causal link between exposure and tumor development *(32)*.

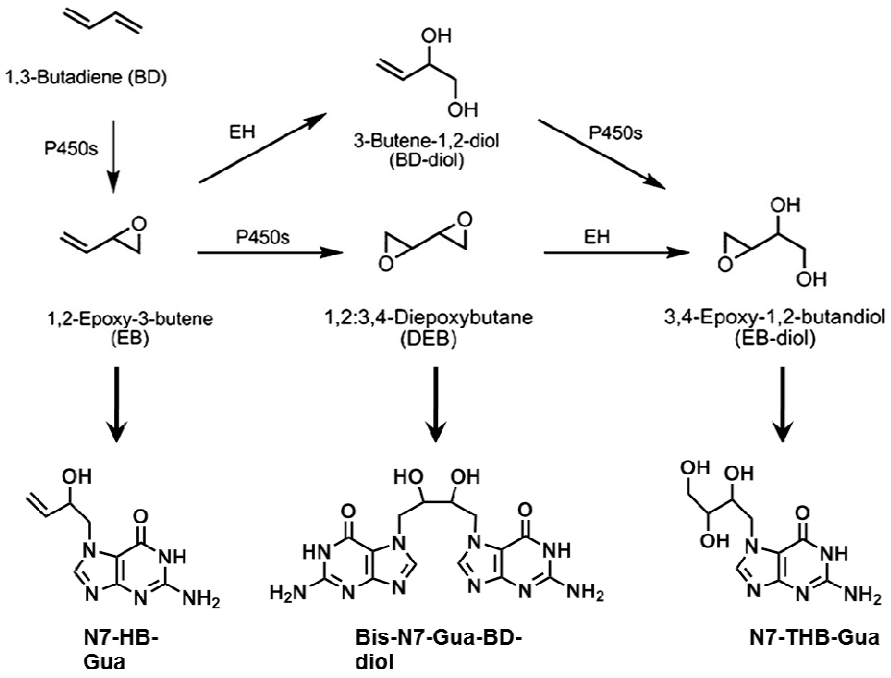

Figure 1: Formation of *N*7-guanine adducts. Shown are *N*7-HB-Gua, bis*N*7-Gua-BD-diol and THB-Gua.

Multiple BD mouse studies have revealed gender differences in the development of neoplasia, Hprt mutant frequencies (MFs), and amounts of DNA adducts formed *(26;27;30).* Inhalation studies in mice revealed pronounced gender differences in sensitivity toward Hprt mutant frequencies (MFs) in BD exposed male and female B6C3F1 mice. Female mice exposed to 1250 ppm BD for 2 weeks demonstrated a 2.3 fold greater number of MFs than male mice *(26)*(Figure 2). In addition, chronic BD inhalation studies in B6C3F1 mice demonstrated male and female mice had tumors of similar tissues, but for the most part, females developed tumors at lower exposure concentrations. For example, lung and liver tumors in female mice were observed at exposure concentrations of 6.25 and 20 ppm BD, respectively. By comparison, the respective exposure concentrations of BD that produced

lung and liver tumors in male mice were 62.5 and 200 ppm *(33)* which represents a 10 fold increase in concentration. There are also gender differences in the formation of *bis*-N7G-BD adduct (a DEB-specific DNA adduct) in male and female B6C3F1 mice exposed to 625 and 200 ppm BD for two weeks. *Bis*-N7G-BD adduct amounts in female mice are 2- to 2.5- fold higher than in male mice *(30)*. Some studies have attributed this gender difference in neoplasia, MFs, and amount of adduct formed to differences in BD metabolism, especially of DEB. However, a recent study of the DEB specific hemoglobin adduct *N,N*-(2,3-dihydroxy-1,4-butadiyl)valine (*pyr*-Val) in mice and rats showed no significant gender differences at the exposure concentrations and durations studied *(34)* . This study would indicate that there is no difference in metabolism of BD and more specifically the highly mutagenic DEB metabolite in female and male rodents at multiple exposure concentrations and durations. An alternative explanation for the multiple gender differences noted above would be a variation in DNA repair pathways for mice and, to a lesser extent, rats. The DNA repair pathway most often linked with BD, and more specifically DEB-induced genotoxic insults is the Fanconi Anemia pathway. The ability of DEB to form DNA interstrand crosslinks is often used as a cellular marker for the diagnosis of Fanconi Anemia disease in suspect non-clinical patients *(35)*. Fanconi anemia (FA) is an inherited genomic instability disorder caused by mutations in genes regulating replication-dependent removal of interstrand DNA crosslinks. The Fanconi Anemia pathway is thought to coordinate a complex mechanism that enlists three classic DNA repair pathways which include homologous recombination, nucleotide excision repair, and mutagenic translesion synthesis *(36)*. Interstrand DNA−DNA adducts are among the most toxic nucleobase lesions because they inhibit DNA replication and transcription, and their enzymatic removal in cells is problematic because of the loss of template

information in both DNA strands. This requires a complex repair process usually involving both nucleotide excision repair and recombination repair, which can lead to DNA rearrangements and deletions *(37)*. Thus, the Fanconi Anemia pathway would be a leading candidate to investigate as the cause of the gender differences in MFs, specific adduct levels, and neoplasm development at differing exposures of BD.

In this study, the molecular dosimetry of DNA adduct formation by BD has been investigated in liver of male and female B6C3F1 mice exposed to 0, 0.1, 0.5, 1.5, 200, or 625 ppm BD by inhalation for 2 weeks and additionally in the liver of female B6C3F1 mice exposed to 0, 1.0, 6.25, or 62.5 BD by inhalation for 2 weeks. We have developed a quantitative high-performance liquid chromatography (HPLC)-electrospray ionization (ESI)-tandem mass spectrometry (MS/MS) methodology for two types of BD induced DNA adducts, N-7-(2,3,4-trihydroxy-3-buten-2-yl)guanine (THB-G, racemic and meso) and N-7-(2-hydroxy-3-buten-1-yl)guanine (HB-G I), and N-7-(1-hydroxy-3-buten-2-yl)guanine (HB-G II). In our approach, the DNA adducts are released from the DNA backbone by neutral thermal hydrolysis, enriched by ultrafiltration and HPLC, and analyzed by either LC/ESI$^+$/MS/MS or nano-LC/ESI$^+$/MS/MS depending upon the exposure, using the [$^{15}N_5$]-labeled adducts as internal standards *(38)*. THB-G and HB-G I and II adducts were chosen for evaluation because the THB-G adducts are formed in much greater amounts compared to other adducts such as the interstrand DNA-DNA cross-links adducts and HB-G. However, even though these N-7 guanine adducts are frequently formed, they have minimal biological relevance since they are chemically unstable and do not participate in Watson-Crick base pairing *(39)*. Nevertheless, it is important to have detailed knowledge of the internal formation of each potentially mutagenic metabolite and its dependence on species, gender,

and exposure concentrations. We report herein a comprehensive exposure-response of N-7 guanine adduct formation observed in the livers of male and female mice that had been exposed to various concentrations of BD by inhalation and the impact of gender on quantification of THB-G and HB-G adducts. Furthermore, we expanded the range of exposure that these N-7 guanine adducts can be accurately measured from a previous low of 20 ppm to 0.5 ppm for THB-G and 62.5 ppm to 6.25 ppm for HB-G using either LC/ESI$^+$/MS/MS or nano-LC/ESI$^+$/MS/MS and greatly lowered the amount of DNA needed for such quantification from 1000 µg to 50 µg for high level exposures and to 300 µg for low level exposure. The majority of this credit for improvement can be given to more sensitive instrumentation and, to a lesser extent, HPLC enrichment of the adducts.

Chapter 2

Materials and Methods

Animals and Treatment

BD inhalation exposures were performed at the Lovelace Respiratory Research Institute (Albuquerque, NM) as previously reported *(30).* Male and female B6C3F1 mice were randomly separated into air-control and exposure groups by weight and were housed individually in hanging wire stainless-steel cages according to NIH guidelines (NIH Publication 86-23; 1985). All procedures involving the use of animals were approved by the Institutional Animal Care and Use Committee. Experimental mice were exposed using multitiered whole-body exposure chambers (H-2000, Laboratory Products). Mice in one chamber received filtered air only as a control group, and mice in the other chamber received nominal 0.1, 0.5, 1.0, 1.5, 6.25, 62.5, 200, or 625 ppm BD for 2 weeks (6 h/d, 5 d/wk). Mice were housed within exposure chambers throughout the experiment and had free access to food and water except for removal of food during the 6-h exposure periods. Within 2 h after cessation of the final day of exposure, mice were euthanized via cardiac puncture, and tissues were harvested and snap-frozen for storage at – 80 ˚C. Tissues were shipped on dry ice to the University of North Carolina at Chapel Hill where they were stored at – 80 ˚C until DNA extraction.

Chemicals

BD (>99%) was acquired from Aldrich Chemical Co. (St. Louis, MO). [$^{15}N_5$]THB-G internal standard and THB-G analyte standard were gifts from Dr. Natalia Tretyakova (University of Minnesota, Minneapolis, MN). [$^{15}N_5$]HB-G I and [$^{15}N_5$]HB-G II internal standards and HB-G I and HB-G II analyte standards were synthesized by the Department of Environmental Sciences and Engineering at the University of North Carolina at Chapel Hill as previously described *(20;31;40).* Nucleic acid purification grade lysis buffer, protein precipitation solution and proteinase K were purchased from Qiagen (Valencia, CA). All other reagents and solvents were purchased from Fisher Scientific.

DNA Isolation

DNA isolation was performed with modification to the Puregene® DNA extraction kit (Qiagen, Valencia, CA) as described previously *(41).* All procedures were performed on ice. Briefly, frozen liver tissue (300-400 mg) was thawed at 4 °C and homogenized in 3 mL Lysis Solution® with a Tehran homogenizer (Wheaton Instruments, Millville, NJ). Following centrifugation, nuclear pellets from homogenates were incubated with a mixture of RNase T1 and RNase A for 30 min at 37 °C, then overnight at 4°C with proteinase K (50 U; Applied Biosystems, Foster City, CA). Protein was precipitated with Protein Precipitation Solution® and centrifugation at 2000 × g for 10 min. The supernatant containing the DNA was transferred to a clean 15 mL tube and precipitated by mixing with 6 mL isopropanol and subsequent centrifugation at 2000 × g for 5 min at 4 °C. The DNA pellet was washed with 6 mL 70% ethanol, centrifuged at 2000 × g for 1 minute at 4 °C, air dried, and resuspended in sterilized double distilled water. DNA purity and amounts were determined by UV spectrophotometry (Shimadzu model UV160U). All A_{260}/A_{280} ratios were between 1.7 and

1.9, ensuring minimal protein contamination and there was no need for DNA reisolation. The DNA solution was stored at -80°C until assayed.

DNA Hydrolysis

Either 50 (for 625 and 200 ppm), 100 (for 62.5 ppm), or 300 (for 6.25, 1.5, 1.0, 0.5, 0.1 and 0 ppm) μg of DNA (depending on exposure level) was used, based on UV measurements, spiked with internal standards, [$^{15}N_5$]THB-G (racemic), [$^{15}N_5$]HB-G I, and [$^{15}N_5$]HB-G II and diluted to 300 μL with HPLC-grade water. The spiked DNA samples were subjected to neutral thermal hydrolysis at 95 ˚C for 30 minutes. Immediately after incubation samples were cooled on ice. The hydrolysates containing the adducts were separated from the DNA backbone by Centricon-10 filtration at 13,500 rpm, 4 ˚C for 45 minutes. After the filtrate was separated, an additional 100 μL HPLC-grade water was added to the retentate to wash the DNA backbone (13,500 rpm, 4 ˚C, 45 minutes) and both filtrates were combined.

High Performance Liquid Chromatography (HPLC)

The samples of hydrolyzed DNA were purified on an Agilent 1200 series HPLC system equipped with a diode-array detector (Santa Clara, CA) and automated fraction collector to separate N-7 guanine adducts from matrix. Separation was performed on a SunFire C18 4.6 × 250 mm 5 μm column (Milford, MA) using a gradient of 10mM ammonium formate (A) in water (adjusted to pH 4.3 with formic acid) and methanol (B). A linear gradient was run from 15% methanol to 30% methanol from 0 to 20 minutes. The flow rate was 1mL/min and the UV absorbance was monitored at 254 nm. Methanol composition was increased linearly to 80% in 2 min; then held at 80% for 6 min, then decreased linearly to 30% in 2 min, then decreased linearly to 15% in 1 min, and held at 15%

for 9 min for column re-equilibration. A 400 μL aliquot of sample was injected. The column oven, autosampler tray and fraction collector chamber temperatures were maintained at 30 °C, 4 °C and 4 °C, respectively. The retention times of THB-G, HB-G I, and HB-G II were ~ 6.5 min, 17 min, and 19 min respectively. Fractions containing the N-7 guanine adducts were automatically collected from 1.5 min before until 1.5 min after its predicted retention time. The fraction collection tubes were placed in a SpeedVac concentrator (ThermoFinnigan, San Jose, CA) and evaporated to dryness. Sample residue was transferred to autosampler vials via 2 x 130 μL washings with 50:50 water:methanol (vol/vol), evaporated to dryness in a SpeedVac concentrator, and finally redissolved in 20 μL HPLC grade water for subsequent analysis by LC-MS/MS.

Quantitation by HPLC-nanoESI$^+$-MS/MS

The quantitative analysis of HB-G I and HB-G II (exposures of 0, 0.1, 0.5, 1.0, 1.5, 6.25, or 62.5 ppm BD) was performed with a nanoAcquity UPLC (Waters, Milford, MA) coupled to a TSQ-Quantum Ultra triple-quadrupole mass analyzer (ThermoFinnigan, San Jose, CA) using the nanospray source in positive mode. The trap column was a Waters 180 μm x 20 mm Symmetry C18 5 μm, and separation was performed on a 100 μm × 100 mm HSS T3 C18 1.8 μm column (Waters, Milford MA). The mobile phase consisted of 0.1% acetic acid in water and acetonitrile. Samples were kept at 4 ˚C during analysis. The sample was first injected onto the trap column at a flow rate of 10 μL per min for 1.5 min at an initial methanol concentration of 5%, then flow was directed in-line with the analytical column. Gradient elution was performed at a flow rate of 600 nL per min. The methanol composition started at 5% and increased linearly to 80% in 10 min, was held at 80% for 2 min, decreased to 5% in 2 min, then held at 5% for 6 min for column re-equilibration. The retention time of

HB-G I and HB-G II was 7.6 min (unable to separate the two isomers), and the total run time was 20 min. The analyte and internal standards were detected in selected reaction monitoring mode (SRM), monitoring the transitions of m/z 222.1 → 152.1 (collision energy 15 eV) for HB-G I and II (analyte) and m/z 227.1 → 157.1 (collision energy 35 eV) for [$^{15}N_5$]HB-G I and II (internal standard). Other nano-electrospray conditions were as follows: positive mode, spray voltage of 2000 V, capillary temperature of 280˚C. The amount of adduct in each sample was calculated from the ratio of the analyte and internal standard peak areas.

Quantitation by HPLC-ESI$^+$-MS/MS

The quantitative analysis of THB-G (all levels of exposure), HB-G I and II (only higher levels of exposure, 200 and 625 ppm BD) was performed with an Acquity UPLC (Waters, Milford, MA) coupled to a TSQ-Quantum Ultra triple-quadrupole mass analyzer (ThermoFinnigan) using heat assisted electrospray ionization (HESI) in positive mode. Samples were kept at 4 ˚C during analysis. Separation was performed on a 2.1 × 100 mm HSS T3 C18, 1.8 μm column (Waters, Milford MA) with gradient elution at a flow rate of 200 μL per min using 0.1% acetic acid in water and methanol. Methanol composition started at 1% and increased linearly to 5% B in 2 min, was held at 5% for 8 min, increased linearly to 80% in 2 min, held at 80% for 2 min, decreased to 1% in 1 min, then held at 1% for 4 min for column re-equilibration. The retention time of THB-G was ~2.9 min, HB-G I ~7.6 min, HB-G II ~7.8 min, and the total run time was 20 min. The analyte and internal standard were detected in Selected Reaction Monitoring (SRM), monitoring the precursor to fragment ion transitions of m/z 256.1 → 152.1 and m/z 261.1 → 157.1 for THB-G and [$^{15}N_5$]THB-G, respectively and m/z 222.1 → 152.1 and m/z 227.1 → 157.1 for HB-G I and II and

[$^{15}N_5$]HB-G I and II, respectively. The electrospray conditions were as follows: positive mode, spray voltage of 3000 V, vaporizer (HESI) temperature of 250°C, sheath gas flow rate 35 (arbitrary units), auxiliary gas flow rate 30 (arbitrary units), capillary temperature of 285°C, and collision energy of 12 eV. The amount of adduct in each sample was calculated from the ratio of the analyte and internal standard peak areas.

Method validation

Method validation was performed by analyzing the analyte standards three times on the same day and on three different days to obtain intraday and interday precision. The intraday and interday precision was defined as the relative standard deviation (RSD) and accuracy was determined by calculating the relative error (RE). Three replicates of control calf thymus DNA (100 μg) were added to HB-G I (5 and 10 μM), or HB-G II (5 and 10 μM), or THB-G (25 and 50 μM) and their corresponding internal standards (100 μM). The validation samples were processed (by neutral thermal hydrolysis, filtration, and fraction collection (HPLC clean-up)) following the same methods as real samples. The intraday precision was determined within one day by analyzing three replicate control samples at concentrations of 5 and 10 μM for HB-G I and II on the HPLC-ESI$^+$-MS/MS and HPLC-nanoESI$^+$-MS/MS and at concentrations of 25 and 50 μM for THB-G on the HPLC-ESI$^+$-MS/MS. The interday precision was determined on three separate days for the control samples.

Statistical Analysis

Statistical analyses were performed using Microsoft Excel spreadsheet analysis tools. A Student's *t* test was used to determine the *P* values for female/male differences in adduct levels.

Chapter 3

Results

Method Validation

The interday and intraday precision and accuracy of the analytical method are listed in Table 1. The RSD of both interday and intraday for HB-G I and HB-G II on the HPLC-nanoESI$^+$-MS/MS were below 6.4%. The accuracies calculated as relative error were within the range of -4.8 to 0.6%. The RSD of both interday and intraday for HB-G I and HB-G II on the HPLC-ESI$^+$-MS/MS were below 8.71%. The accuracies calculated as relative error were within the range of -5.8 to 1.8%. The RSD of both interday and intraday for THB-G on the HPLC-ESI$^+$-MS/MS were below 9.06%. The accuracies calculated as relative error were within the range of -10.8 to -5.0%. For the HPLC-ESI$^+$-MS/MS, the limit of detection (LOD) with a signal-to-noise of >2 was 3 fmol THB-G standard per injection; therefore, the limit of quantitation (LOQ) was set to be three times the LOD (9 fmol of THB-G per injection) with a signal-to-noise of > 6. The LOD with a signal-to-noise of >2 was 1 fmol HB-G I and HB-G II standard per injection; therefore, the LOQ was set to be three times the LOD (3 fmol of HB-G I and HB-G II per injection) with a signal-to-noise of > 6. For the HPLC-nanoESI$^+$-MS/MS, the LOD with a signal-to-noise of >2 was 500 amol HB-G I and HB-G II standard per injection; therefore, the LOQ was set to be three times the LOD (1.5 fmol of HB-G I and HB-G II per injection) with a signal-to-noise of > 6. The lower detection

limit for HB-G adducts compared to that for THB-G adducts was attributed to a higher sensitivity of ESI+/MS/MS detection for HB-G adducts.

HPLC-nanoESI$^+$-MS/MS								
Adduct	Intraday (n=3)				Interday (n=3)			
HB-G I	Concentration (uM)	Determined concentration (uM)	Precision (%RSD)	Accuracy (%RE)	Concentration (uM)	Determined concentration (uM)	Precision (%RSD)	Accuracy (%RE)
	10.0	9.81 ± 0.17	1.73	-1.9	10.0	9.79 ± 0.21	2.14	-2.1
	5.00	5.03 ± 0.30	5.96	0.6	5.00	4.84 ± 0.31	6.4	-3.2
Adduct	Intraday (n=3)				Interday (n=3)			
HB-G II	Concentration (uM)	Determined concentration (uM)	Precision (%RSD)	Accuracy (%RE)	Concentration (uM)	Determined concentration (uM)	Precision (%RSD)	Accuracy (%RE)
	10.0	9.96 ± 0.15	1.51	-1.1	10.0	9.65 ± 0.24	2.48	-3.5
	5.00	5.00 ± 0.22	4.40	0.0	5.00	4.76 ± 0.28	5.88	-4.8
HPLC-ESI$^+$-MS/MS								
Adduct	Intraday (n=3)				Interday (n=3)			
HB-G I	Concentration (uM)	Determined concentration (uM)	Precision (%RSD)	Accuracy (%RE)	Concentration (uM)	Determined concentration (uM)	Precision (%RSD)	Accuracy (%RE)
	10.0	9.77 ± 0.12	1.21	-1.1	10.0	9.73 ± 0.37	3.8	-2.7
	5.00	5.09 ± 0.25	4.91	1.8	5.00	4.71 ± 0.41	8.7	-5.8
Adduct	Intraday (n=3)				Interday (n=3)			
HB-G II	Concentration (uM)	Determined concentration (uM)	Precision (%RSD)	Accuracy (%RE)	Concentration (uM)	Determined concentration (uM)	Precision (%RSD)	Accuracy (%RE)
	10.0	9.82 ± 0.14	1.42	-1.8	10.0	9.80 ± 0.44	4.49	-2.0
	5.00	4.88 ± 0.19	3.89	-2.4	5.00	4.82 ± 0.42	8.71	-3.6
Adduct	Intraday (n=3)				Interday (n=3)			
THB-G	Concentration (uM)	Determined concentration (uM)	Precision (%RSD)	Accuracy (%RE)	Concentration (uM)	Determined concentration (uM)	Precision (%RSD)	Accuracy (%RE)
	50.0	46.81 ± 1.77	3.84	-6.4	50.0	47.52 ± 2.34	4.92	-5.0
	25.00	23.38 ± 1.37	5.85	-6.5	25.00	22.29 ± 2.02	9.06	-10.8

Table 1: Intraday and interday accuracy and precision

[$^{15}N_5$]THB-G (racemic) was used as the internal standard for both the racemic and meso THB-Gua (44). The response was linear for both THB-Gua and HB-Gua adducts over the working range (5-100 fmol injected) with R^2 values of ≥0.997. Typical 5-point calibration curves for HB-Gua II and THB-Gua are given in Figures 3 and 4 respectively. A typical set of product ion chromatograms of the adducts and their internal standards is given in Figure 5 for THB-G and HB-G I and HB-G II on the HPLC-ESI$^+$-MS/MS and Figure 6 for HB-G on the HPLC-nanoESI$^+$-MS/MS.

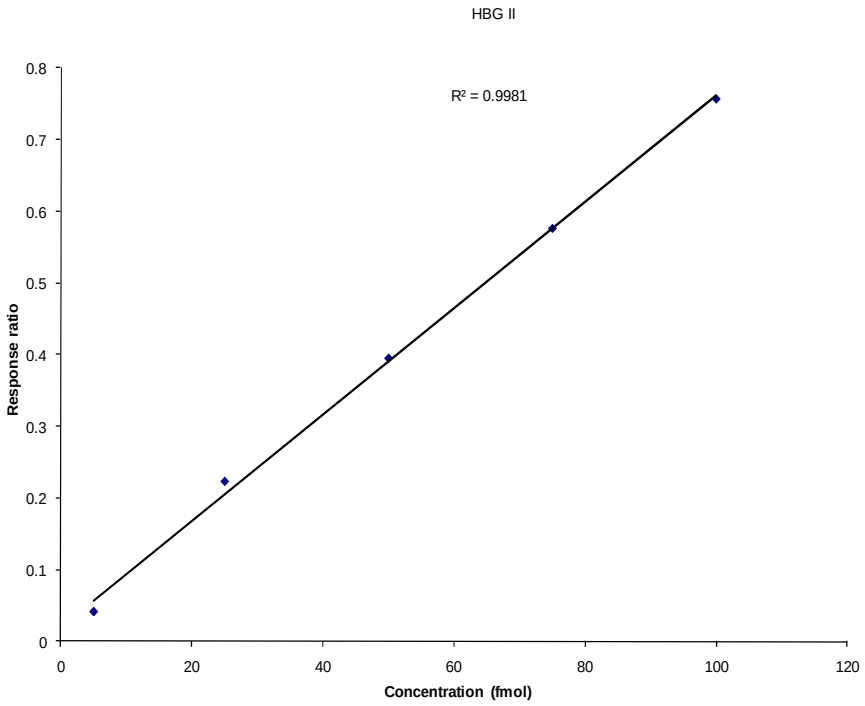

Figure 3: Calibration Curve for HB-G II

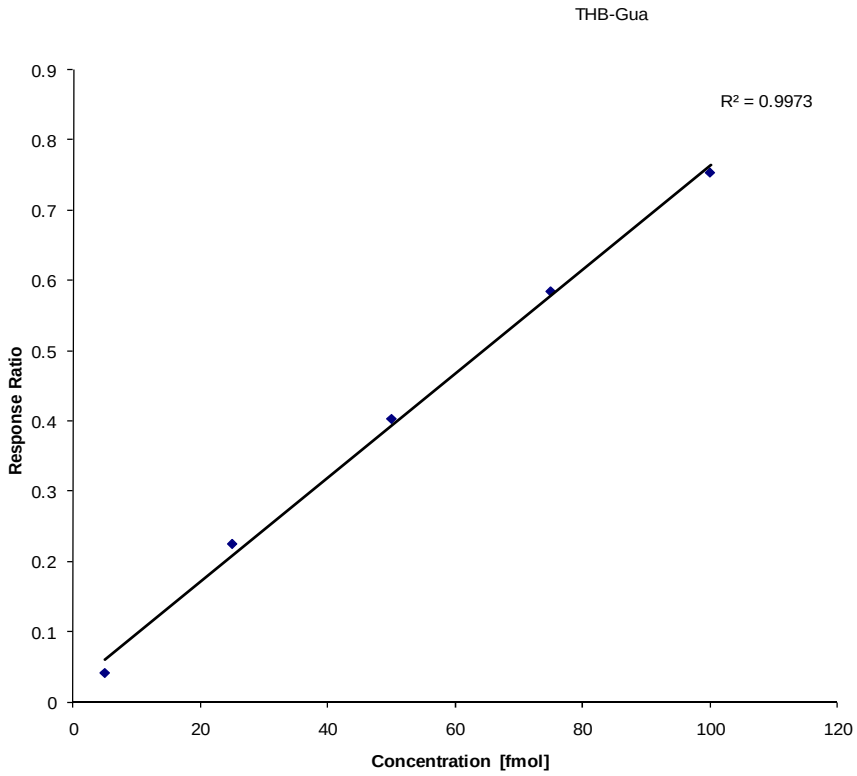

Figure 4: Calibration Curve for THB-G

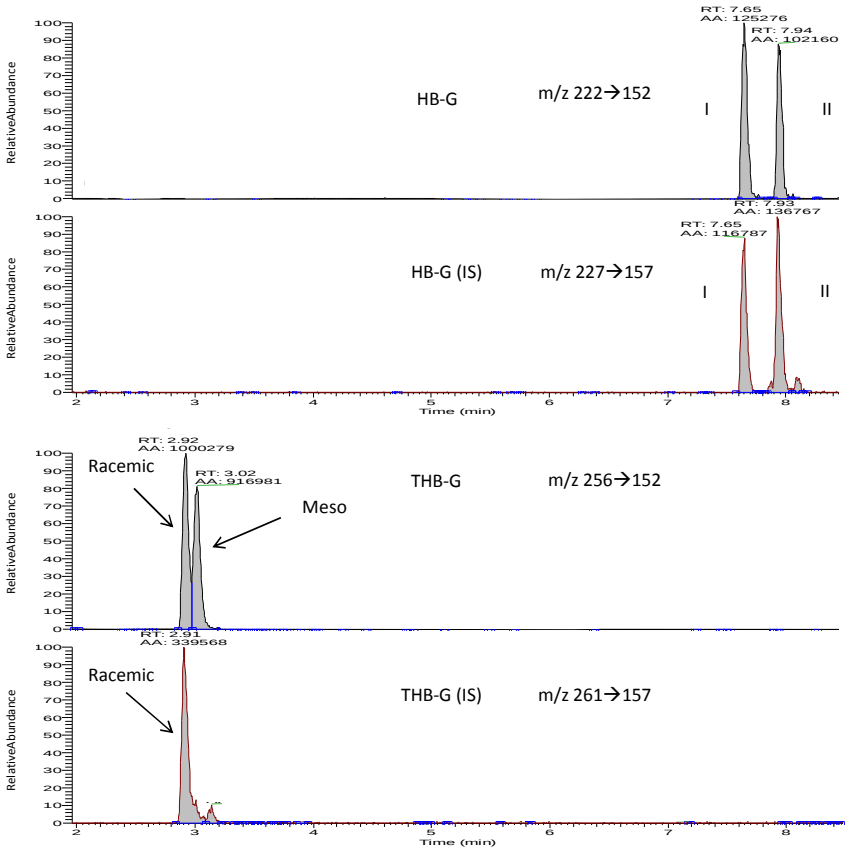

Figure 5: Chromatogram of 625 ppm THB-G and HB-G I & II Adducts

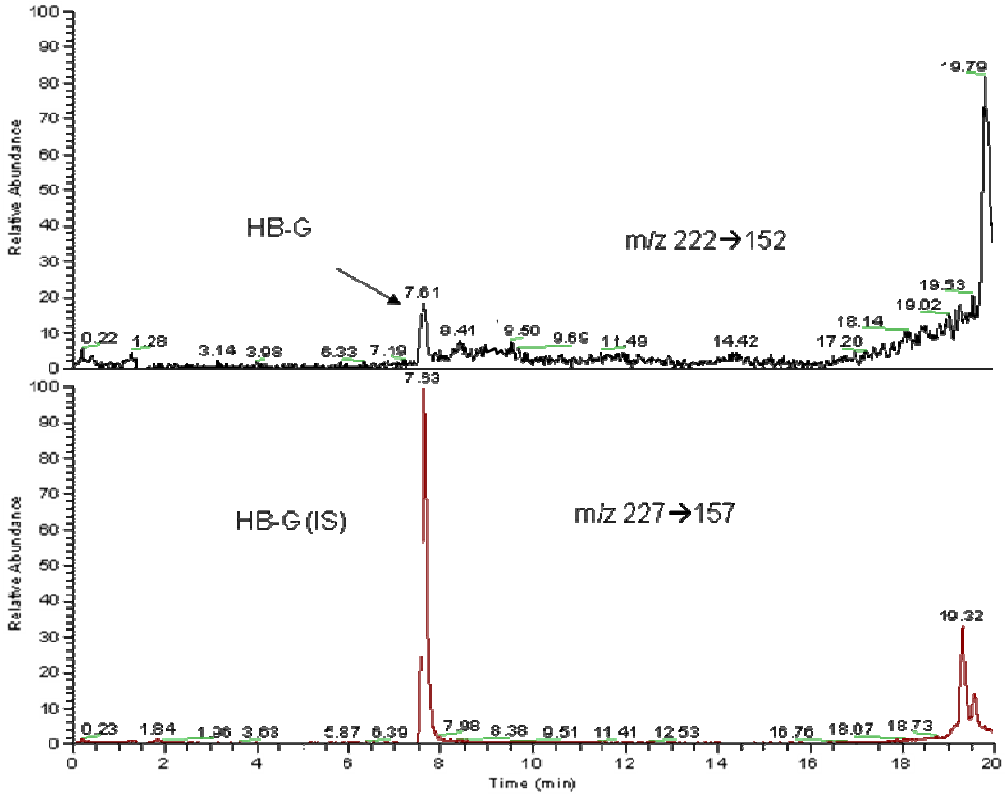

Figure 6: Chromatogram of 6.25 ppm HB-G adduct

Molecular Dosimetry of THB-Gua and HB-Gua Adducts

Table 2 shows the number of HB-G and THB-G adducts per 10^8 unmodified guanine bases in liver from mice exposed by inhalation to 0, 0.1, 0.5, 1.0, 1.5, 6.25, 62.5, 200, and 625 ppm BD for 2 weeks. Both female and male B6C3F1 mice exhibited a supralinear dose response in the formation of THB-G and a linear dose response in the formation of HB-G adducts (Figures 7, 8, and 9). Figures 7 and 8 illustrates the exposure-response data for THB-G DNA adducts in male and female mice. The dose response curves for THB-G in both genders are supralinear, providing evidence for partial saturation of metabolic activation pathways in mice at exposures to >200 ppm BD. The THB-G adducts were detectable down

to a level of 0.5 ppm due to their greater extent of formation. Figure 9 illustrates the exposure-response data for HB-G DNA adducts in male and female mice. In contrast to THB-G, the dose response curves are curvilinear and do not show any signs of metabolic saturation. The amounts of HB-G adducts were approximately 10-20 fold lower than THB-G adducts. Detection was usually at or slightly above the LOD for HB-G in samples from the 6.25 ppm exposure group because of their presence in very low amounts. Overall, there was no statistically significant gender difference ($p < 0.05$) in the number of adducts at exposures where both male and female mice were analyzed (See Figures 10 – 15). The amounts of THB-G adducts were always higher than those of HB-G adducts in liver tissue.

	HB Gua				THB-Gua			
Dose	*n*	**Males**	*n*	**Females**	*n*	**Males**	*n*	**Females**
0	14	ND	10	ND	14	ND	10	ND
0.1	8	ND	8	ND	8	ND	8	ND
0.5	8	ND	5	ND	8	9.56 ± 1.52	5	8.34 ± 1.54
1	0	N/A	5	ND	0	N/A	5	17.1 ± 1.6
1.5	9	ND	6	ND	9	35.3 ± 6.65	6	31.6 ± 3.64
6.25	0	N/A	5	8.3 ± 4.9	0	N/A	5	70.1 ± 8.7
62.5	0	N/A	5	29 ± 11	0	N/A	5	732 ± 150
200	11	122 ± 20	8	138 ± 12	11	3914 ± 682	8	3635 ± 353
625	8	659 ± 85	5	728 ± 94	8	6205 ± 824	5	6103 ± 1140

Table 2: Amounts of BD-induced N-7 guanine adducts in female and male B6C3F1 mice

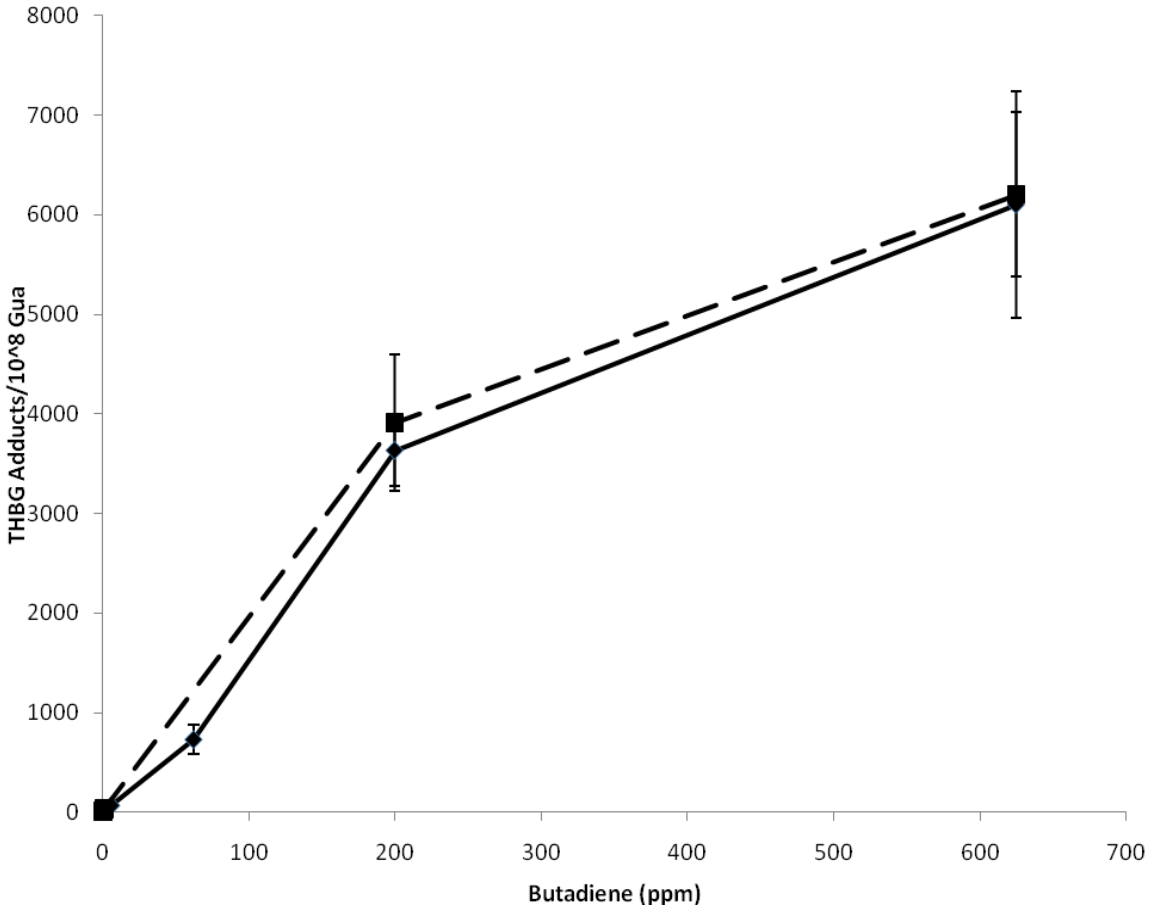

Figure 7: Exposure-response relationship of the formation of THBG in liver; Female mice were denoted by a solid black line and male mice were denoted by a dashed black line.

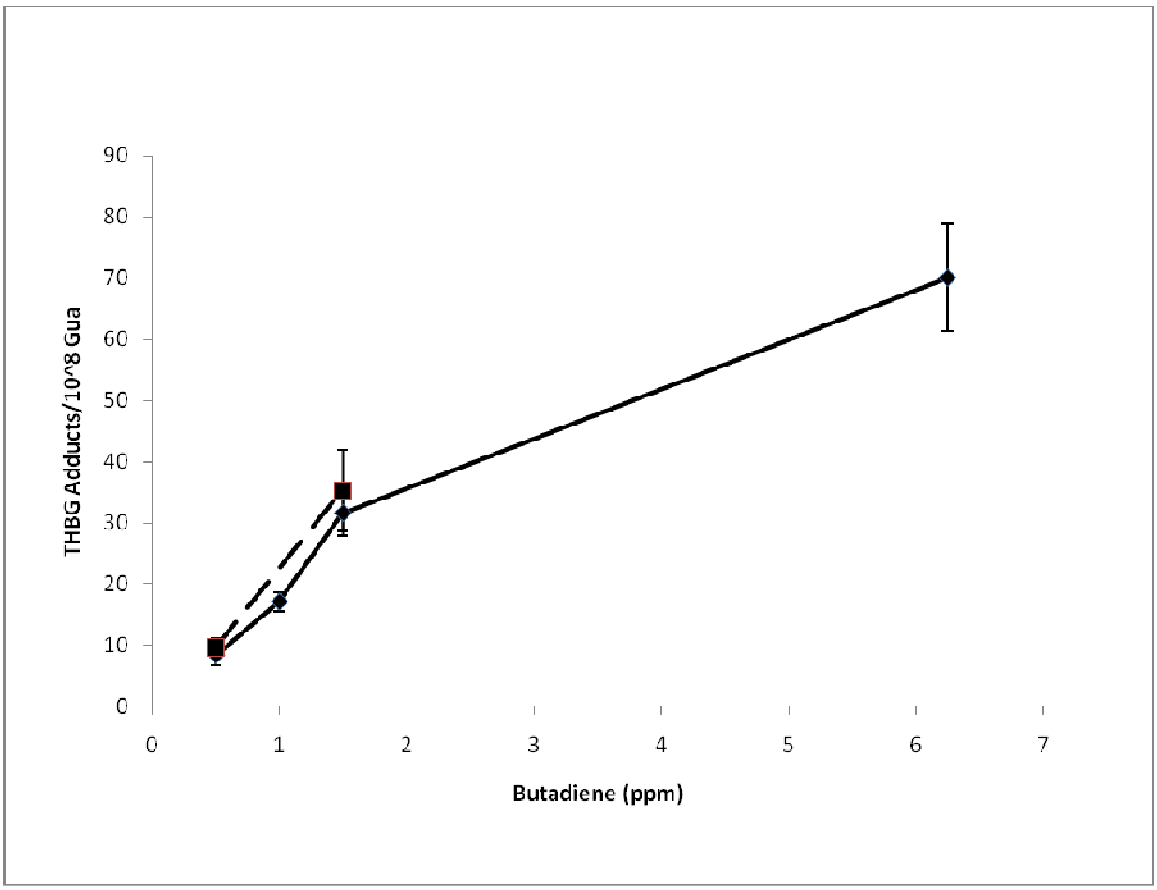

Figure 8: Exposure-response relationship of the formation of THBG in liver from exposure levels of 0.5 ppm to 6.25 ppm butadiene; Female mice were denoted by a solid black line and male mice were denoted by a dashed black line.

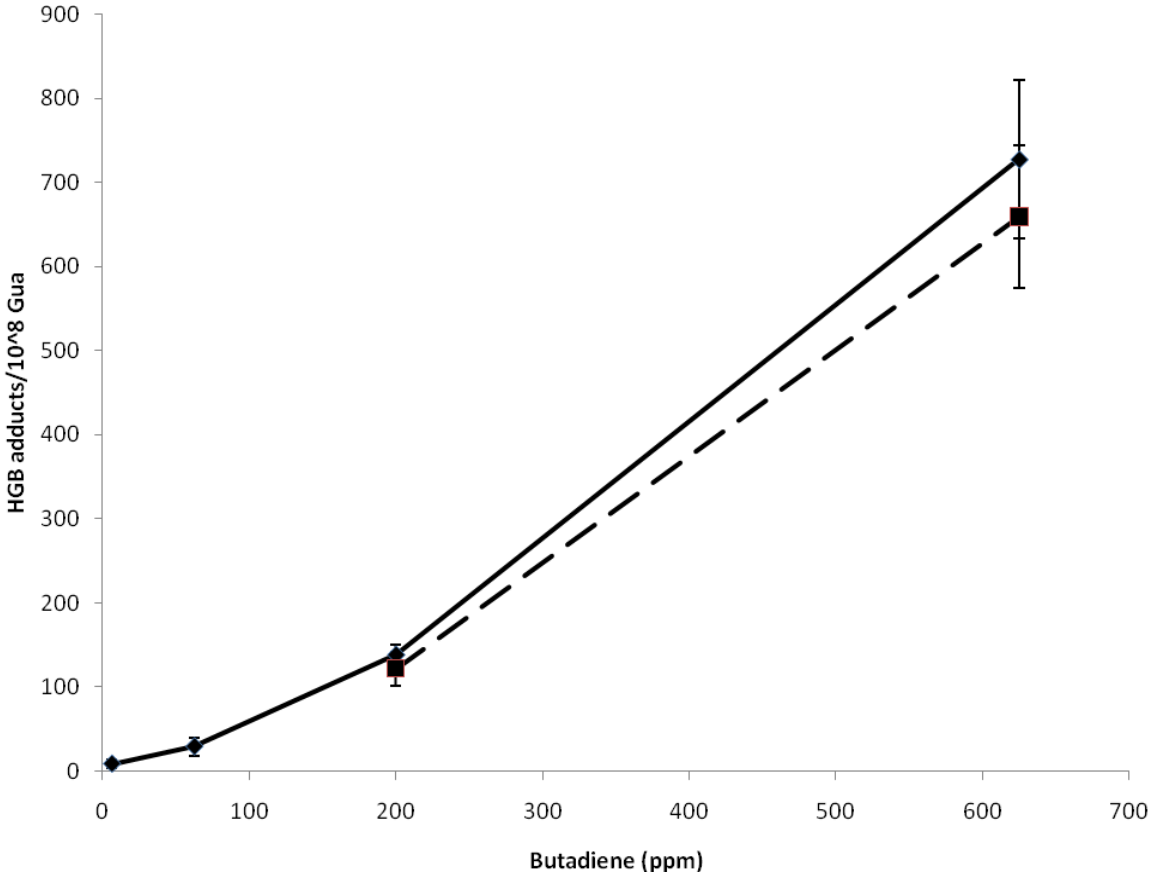

Figure 9: Exposure-response relationship of the formation of HBG in liver; Female mice were denoted by a solid black line and male mice were denoted by a dashed black line.

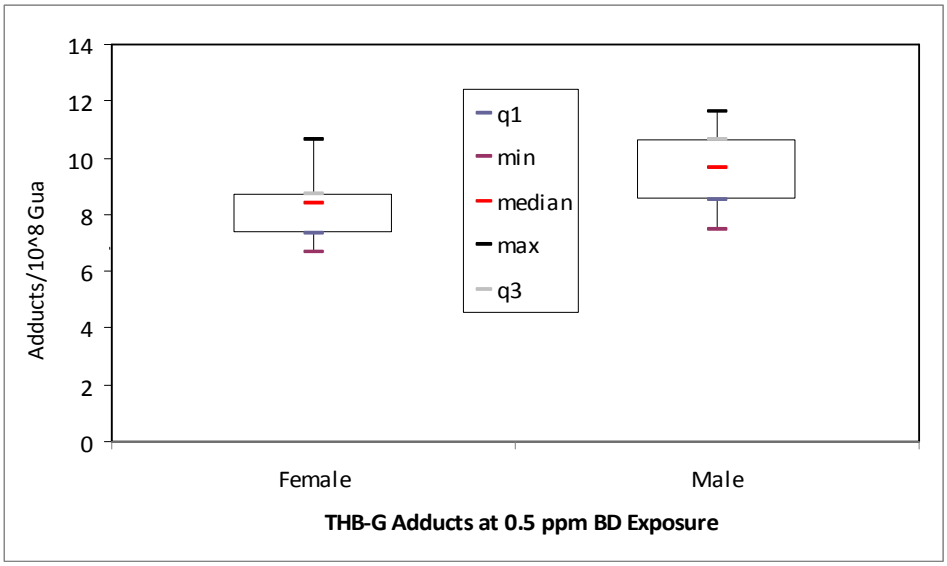

Figure 10: Comparison of Butadiene induced THB-G adducts in female and male B6C3F1 mice at exposure concentration of 0.5 ppm 1,3-butadiene

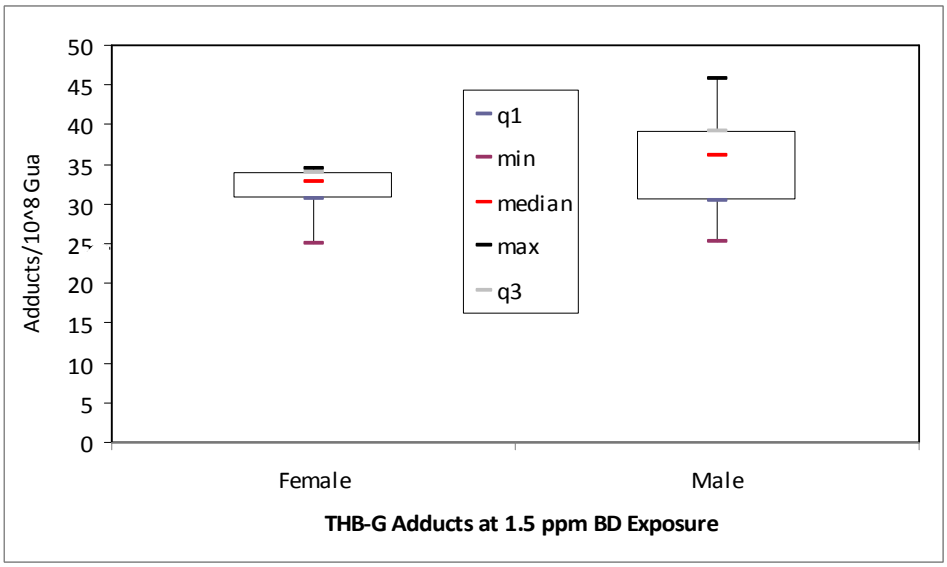

Figure 11: Comparison of Butadiene induced THB-G adducts in female and male B6C3F1 mice at exposure concentration of 1.5 ppm 1,3-butadiene

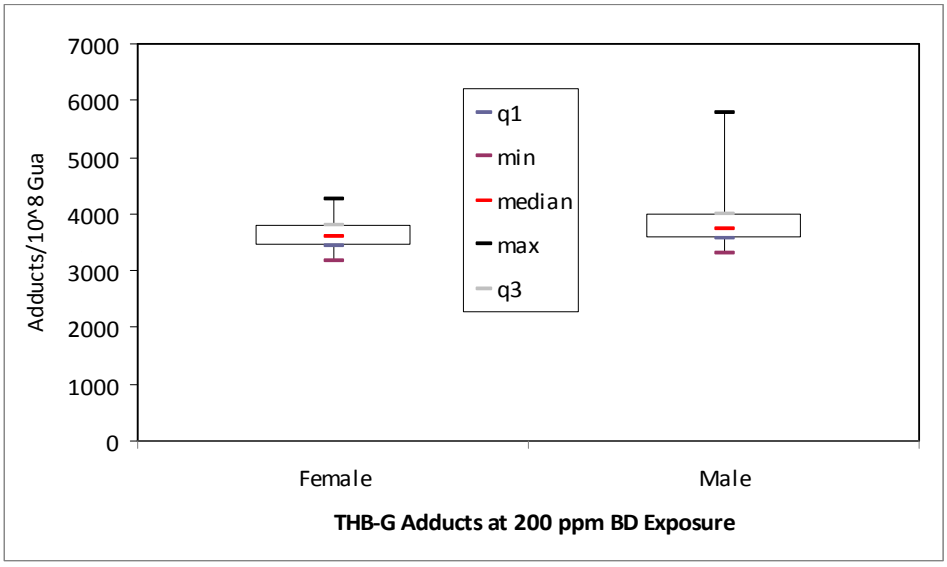

Figure 12: Comparison of Butadiene induced THB-G adducts in female and male B6C3F1 mice at exposure concentration of 200 ppm 1,3-butadiene

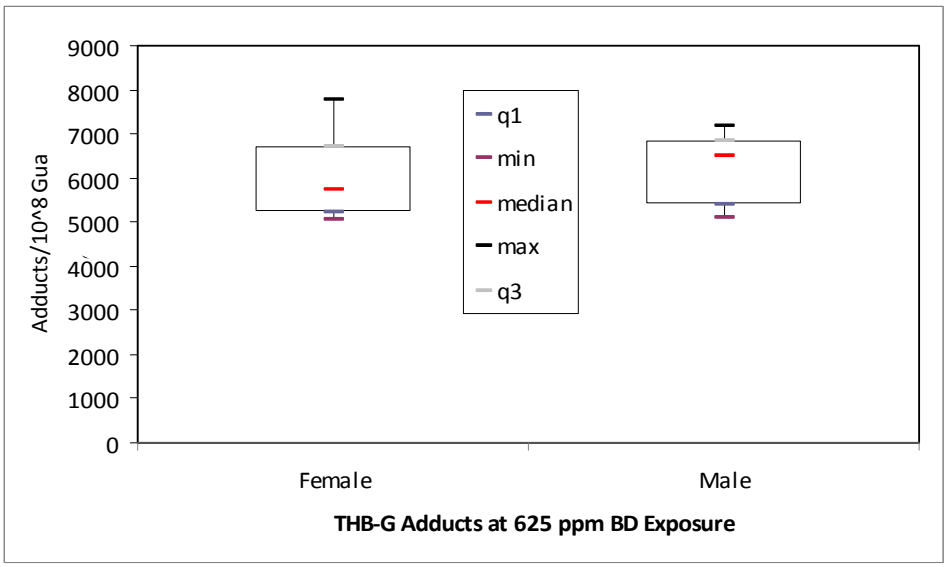

Figure 13: Comparison of Butadiene induced THB-G adducts in female and male B6C3F1 mice at exposure concentration of 625 ppm 1,3-butadiene

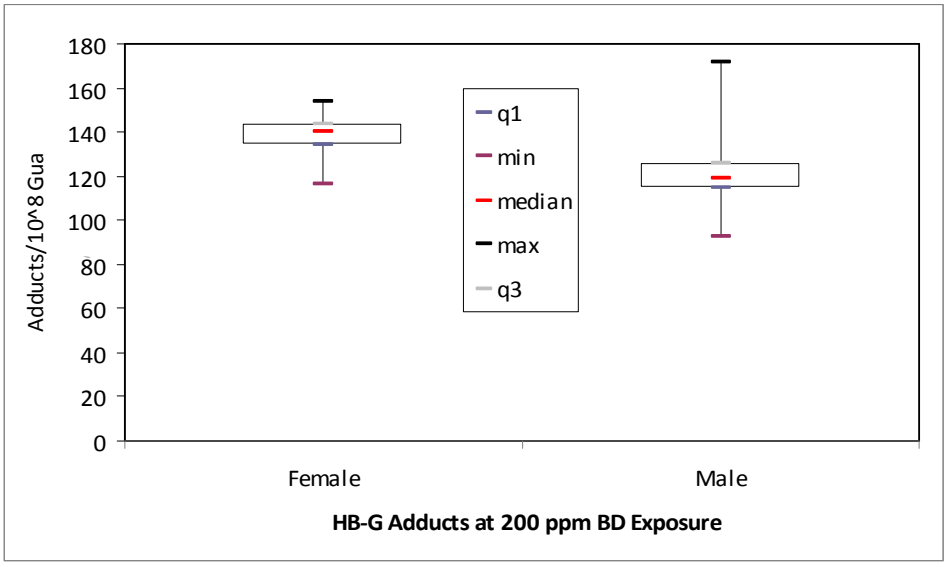

Figure 14: Comparison of Butadiene induced HB-G adducts in female and male B6C3F1 mice at exposure concentration of 200 ppm 1,3-butadiene.

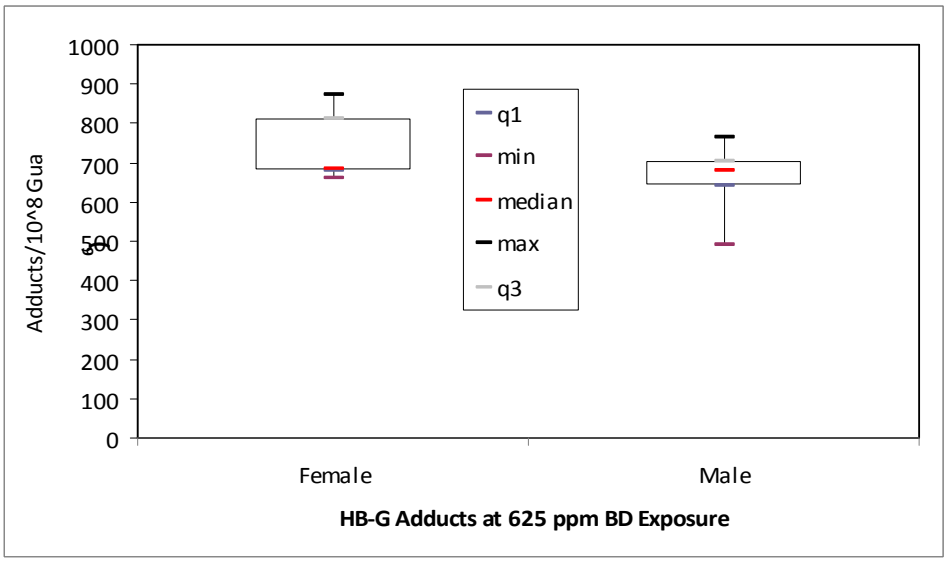

Figure 15: Comparison of Butadiene induced HB-G adducts in female and male B6C3F1 mice at exposure concentration of 625 ppm 1,3-butadiene.

Chapter 4

Discussion

The main purpose of this work was to study the molecular dosimetry of the N-7 guanine adducts of BD to determine any gender differences in mice. The quantitation method used in this study is highly specific and reliable for the quantitation of N-7 guanine adducts because of the following: (i) the neutral thermal hydrolysis process allowed selective depurination of the N-7 guanine adducts, compared to guanine. (ii) Other sources of interference (i.e., guanine and adenine) were removed by HPLC fraction collection. (iii) The MS/MS detection allowed specific identification of the product ions originating from the protonated adducts. (iv) Finally, the use of internal standards corrected for losses in sample processing starting with hydrolysis of DNA. The method has good sensitivity; however, detection of HB-G was challenging at low BD exposures due to the presence of these adducts in very small amounts, rather than to a lack of sensitivity in the method.

This study is the first report of the relationships between exposure and the molecular dose of THB-G and HB-G adducts in female and male mice. There were no gender differences in the amounts of adduct formed at levels of exposure where data was available for both sexes. This data is in agreement with the study by Georgieva et al., *(34)* where the DEB-specific hemoglobin adduct (*pyr*-Val) also showed no gender differences in male and female mice and rats. Taken together, these results confirm that BD metabolism in male and female mice is comparable. The similarity in the amounts of N-7 guanine adducts among

male and female mice would not be expected on the basis of previous reports of BD carcinogenicity, MFs, and other DNA adducts *(6;30;42)*. However, no gender differences were found in globin adducts of the three epoxides *(43)*.The lowest level that THB-G adducts were quantifiable was 0.5 ppm butadiene for 2 weeks. The lowest level that HB-G adducts were quantifiable was 6.25 ppm butadiene for 2 weeks. While these N7-guanine adducts are frequently formed, they have minimal biological relevance due to their chemical instability and their inability to interfere with Watson Crick base pairings *(39)*. The majority of N7-guanine adducts are hydrolytically unstable, as N-7 alkylation of guanine produces a positive charge on the modified nucleobase and destabilizes the β-glycosidic bond, leading to spontaneous depurination and formation of abasic sites. Even though N7-guanine adducts undergo spontaneous depurination resulting in apurinic sites (a potential source of mutation), these are efficiently repaired, so that they do not cause any increase over the endogenous number of AP sites *(44)*. Consequently, it is highly unlikely that THB-G and HB-G adducts are the cause of the mutations seen in BD-induced carcinogenesis. Furthermore, since gender based data suggests that bis-N7G-BD is the primary adduct initiating mutagenesis and carcinogenesis, and does show a sex linked increase in females; THB-G and HB-G can be eliminated as playing a significant role in genotoxicity, mutagenesis, and rodent carcinogenesis. Nevertheless, the significance of this study demonstrates that there were no gender differences in the amounts of THB-G and HB-G adducts formed at exposures where data was available for both sexes. Consequently, there is no gender difference in BD metabolism.

Because of the similarity in the numbers of adducts, the exposure−response curves were also similar for male and female mice. The nonlinear response for THB-Gua in both

mice genders suggests partial saturation of metabolic activation starting at 200 ppm. The HB-Gua adducts, on the other hand, appeared to have linear exposure−response relationships, although it was harder to make this conclusion because of relatively high standard deviations for HB-G adduct values at low levels of exposure. The fact that THB-G adduct formation exhibits partial saturation at 200 ppm, but HB-G continues to increase linearly, suggests that the primary source of THB-G is EBD that was primarily converted from BD-diol.

This research has demonstrated an important similarity and no differences between DNA adducts and BD metabolites in male and female mice. It also raises an important question related to BD carcinogenicity. If metabolism of BD in male and female mice is the same, what explains the gender differences seen in MFs, specific DEB induced DNA adducts, and lower levels of BD needed to induce neoplasia in female mice compared to male mice? *Pyr*-Val data and the HB-G and THB-G adduct data from this paper indicate that there is no difference in BD metabolism in female and male mice at multiple exposure concentrations and durations. This comprehensive data set strongly suggests that a deficiency in DNA cross-link repair in females is the most plausible hypothesis for the gender differences in mutagenic and carcinogenic susceptibility. Although not investigated in the present work, the Fanconi Anemia pathway, while complicated, represents possible targets for the gender-specific repair pathway responsible for these discrepancies. FA cells have been shown to be hypersensitive to DEB. However, a possible involvement of this recombination repair pathway in the protection of cells against DEB-induced DNA damage remains to be explored using transgenic animals.

References

(1) White, W. C. (2007) Butadiene production process overview. *Chem. Biol. Interact.* **166,** 10-14.

(2) Pelz, N., Dempster, N. M., and Shore, P. R. (1990) Analysis of low molecular weight hydrocarbons including 1,3-butadiene in engine exhaust gases using an aluminum oxide porous-layer open-tubular fused-silica column. *J. Chromatogr. Sci.* **28,** 230-235.

(3) Hecht, S. S. (1999) Tobacco smoke carcinogens and lung cancer. *J. Natl. Cancer Inst.* **91,** 1194-1210.

(4) Fowles, J., and Dybing, E. (2003) Application of toxicological risk assessment principles to the chemical constituents of cigarette smoke. *Tob. Control* **12,** 424-430.

(5) US Environmental Protection Agency (2002) Health Assessment of 1,3-Butadiene. National Center for Environmental Assessment, Washington, DC.

(6) IARC. (2008) 1,3-butadiene, ethylene oxide and vinyl halides (vinyl fluoride, vinyl chloride and vinyl bromide). *IARC Monogr. Eval. Carcinog. Risks Hum.* **97,** 1-287.

(7) Santos-Burgoa, C., Matanoski, G. M., Zeger, S., and Schwartz, L. (1992) Lymphohematopoietic cancer in styrene-butadiene polymerization workers. *Am. J. Epidemiol.* **136,** 843-854.

(8) Divine, B. J., Wendt, J. K., and Hartman, C. M. (1993) Cancer mortality among workers at a butadiene production facility. *IARC Sci. Publ.* 345-362.

(9) Delzell, E., Sathiakumar, N., Hovinga, M., Macaluso, M., Julian, J., Larson, R., Cole, P., and Muir, D. C. (1996) A follow-up study of synthetic rubber workers. *Toxicology* **113,** 182-189.

(10) Macaluso, M., Larson, R., Delzell, E., Sathiakumar, N., Hovinga, M., Julian, J., Muir, D., and Cole, P. (1996) Leukemia and cumulative exposure to butadiene, styrene and benzene among workers in the synthetic rubber industry. *Toxicology* **113,** 190-202.

(11) Huff, J. E., Melnick, R. L., Solleveld, H. A., Haseman, J. K., Powers, M., and Miller, R. A. (1985) Multiple organ carcinogenicity of 1,3-butadiene in B6C3F1 mice after 60 weeks of inhalation exposure. *Science* **227,** 548-549.

(12) Melnick, R. L., and Huff, J. (1992) 1,3-Butadiene: Toxicity and carcinogenicity in laboratory animals and in humans. *Rev. Environ. Contam. Toxicol.* **124,** 111-144.

(13) Owen, P. E., Glaister, J. R., Gaunt, I. F., and Pullinger, D. H. (1987) Inhalation toxicity studies with 1,3-butadiene 3 Two year toxicity/carcinogenicity study in rats. *Am. Indus. Hyg. Assoc. J.* **48,** 407-413.

(14) Elfarra, A. A., Moll, T. S., Krause, R. J., Kemper, R. A., and Selzer, R. R. (2001) Reactive metabolites of 1,3-butadiene: DNA and hemoglobin adduct formation and potential roles in carcinogenicity. *Adv. Experim. Med. Biol.* **500,** 93-103.

(15) Himmelstein, M. W., Turner, M. J., Asgharian, B., and Bond, J. A. (1996) Metabolism of 1,3-butadiene: Inhalation pharmacokinetics and tissue dosimetry of butadiene epoxides in rats and mice. *Toxicology* **113,** 306-309.

(16) Csanády, G. A., Guengerich, F. P., and Bond, J. A. (1992) Comparison of the biotransformation of 1,3-butadiene and its metabolite, butadiene monoepoxide, by hepatic and pulmonary tissues from humans, rats and mice. *Carcinogenesis* **13,** 1143-1153.

(17) Duescher, R. J., and Elfarra, A. A. (1992) 1,3-Butadiene oxidation by human myeloperoxidase: role of chloride ion in catalysis of divergent pathways. *J. Biol. Chem.* **267,** 19859-19865.

(18) Duescher, R. J., and Elfarra, A. A. (1994) Human liver microsomes are efficient catalysts of 1,3-butadiene oxidation: evidence for major roles by cytochromes P450 2A6 and 2E1. *Arch. Biochem. Biophys.* **311,** 342-349.

(19) Krause, R. J., and Elfarra, A. A. (1997) Oxidation of butadiene monoxide to *meso*- and (±)-diepoxybutane by cDNA-expressed human cytochrome P450s and by mouse, rat, and human liver microsomes: evidence for preferential hydration of *meso*-diepoxybutane in rat and human liver microsomes. *Arch. Biochem. Biophys.* **337,** 176-184.

(20) Tretyakova, N. Y., Lin, Y. P., Upton, P. B., Sangaiah, R., and Swenberg, J. A. (1996) Macromolecular adducts of butadiene. *Toxicology* **113,** 70-76.

(21) Swenberg, J. A., Koc, H., Upton, P. B., Georgieva, N., Ranasinghe, A., Walker, V. E., and Henderson, R. (2001) Using DNA and hemoglobin adducts to improve the risk assessment of butadiene. *Chem. -Biol. Interact.* **135-136,** 387-403.

(22) Gervasi, P. G., Citti, L., Del Monte, M., Longo, V., and Benetti, D. (1985) Mutagenicity and chemical reactivity of epoxidic intermediates of the isoprene metabolism and other structurally related compounds. *Mutat. Res.* **156,** 77-82.

(23) Tice, R. R., Boucher, R., Luke, C. A., and Shelby, M. D. (1987) Comparative cytogenetic analysis of bone marrow damage induced in male B6C3F1 mice by multiple exposures to gaseous 1,3-butadiene. *Environ. Mutagen.* **9,** 235-250.

(24) Cochrane, J. E., and Skopek, T. R. (1994) Mutagenicity of butadiene and its epoxide metabolites: I. Mutagenic potential of 1,2-epoxybutene, 1,2,3,4-diepoxybutane and 3,4-epoxy-1,2-butanediol in cultured human lymphoblasts. *Carcinogenesis* **15,** 713-717.

(25) Cochrane, J. E., and Skopek, T. R. (1994) Mutagenicity of butadiene and its epoxide metabolites: II. Mutational spectra of butadiene, 1,2-epoxybutene and diepoxybutane at the *hprt* locus in splenic T cells from exposed B6C3F1 mice. *Carcinogenesis* **15,** 719-723.

(26) Meng, Q., Redetzke, D. L., Hackfeld, L. C., Hodge, R. P., Walker, D. M., and Walker, V. E. (2007) Mutagenicity of stereochemical configurations of 1,2-epoxybutene and 1,2:3,4-diepoxybutane in human lymphblastoid cells. *Chem. -Biol. Interact.* **166,** 207-218.

(27) Walker, V. E., Walker, D. M., Meng, Q., McDonald, J. D., Scott, B. R., Bauer, M. J., Seilkop, S. K., Claffey, D. J., Upton, P. B., Powley, M. W., Swenberg, J. A., and Henderson, R. F. (2009) Genotoxicity of 1,3-butadiene and its epoxy intermediates. Health Effects Institute, Capital City Press, Montpelier, VT.

(28) Park, S., and Tretyakova, N. (2004) Structural characterization of the major DNA-DNA cross-link of 1,2,3,4-diepoxybutane. *Chem. Res. Toxicol.* **17,** 129-136.

(29) Zhang, X. Y., and Elfarra, A. A. (2005) Reaction of 1,2,3,4-diepoxybutane with 2'-deoxyguanosine: initial products and their stabilities and decomposition patterns under physiological conditions. *Chem. Res Toxicol.* **18,** 1316-1323.

(30) Goggin, M., Swenberg, J. A., Walker, V. E., and Tretyakova, N. (2009) Molecular dosimetry of 1,2,3,4-diepoxybutane-induced DNA-DNA cross-links in B6C3F1 mice and F344 rats exposed to 1,3-butadiene by inhalation. *Cancer Res.* **69,** 2479-2486.

(31) Tretyakova, N. Y., Sangaiah, R., Yen, T. Y., and Swenberg, J. A. (1997) Synthesis, characterization, and *in vitro* quantitation of *N*-7-guanine adducts of diepoxybutane. *Chem. Res. Toxicol.* **10,** 779-785.

(32) Preston, R. J. (2007) Cancer risk assessment for 1,3-butadiene: Data integration opportunities. *Chem. -Biol. Interact.* **166,** 150-155.

(33) National Toxicology Program (1993) Toxicology and carcinogenesis studies of 1,3-butadiene in B6C3F1 mice (inhalation studies). pp 1-319, US Public Health Service, US Department of Health and Human Services, Research Triangle Park, NC.

(34) Georgieva, N. I., Boysen, G., Bordeerat, N., Walker, V. E., and Swenberg, J. A. (2010) Exposure-Response of 1,2:3,4-Diepoxybutane Specific N-Terminal Valine Adducts in Mice and Rats after Inhalation Exposure to 1,3-Butadiene. *Toxicol. Sci.*

(35) Auerbach, A. D. (2009) Fanconi anemia and its diagnosis. *Mutat. Res* **668,** 4-10.

(36) Moldovan, G. L., and D'Andrea, A. D. (2009) How the fanconi anemia pathway guards the genome. *Annu. Rev. Genet.* **43,** 223-249.

(37) Zheng, H., Wang, X., Warren, A. J., Legerski, R. J., Nairn, R. S., Hamilton, J. W., and Li, L. (2003) Nucleotide excision repair- and polymerase eta-mediated error-prone removal of mitomycin C interstrand cross-links. *Mol. Cell Biol.* **23,** 754-761.

(38) Koc, H., Tretyakova, N. Y., Walker, V. E., Henderson, R. F., and Swenberg, J. A. (1999) Molecular dosimetry of N-7 guanine adduct formation in mice and rats exposed to 1,3-butadiene. *Chem. Res. Toxicol.* **12,** 566-574.

(39) Boysen, G., Pachkowski, B. F., Nakamura, J., and Swenberg, J. A. (2009) The formation and biological significance of N7-guanine adducts. *Mutat. Res* **678,** 76-94.

(40) Tretyakova, N., Lin, Y., Sangaiah, R., Upton, P. B., and Swenberg, J. A. (1997) Identification and quantitation of DNA adducts from calf thymus DNA exposed to 3,4-epoxy-1-butene. *Carcinogenesis* **18,** 137-147.

(41) Morinello, E. J., Ham, A. J. L., Ranasinghe, A., Nakamura, J., Upton, P. B., and Swenberg, J. A. (2002) Molecular dosimetry and repair of N^2,3-ethenoguanine in rats exposed to vinyl chloride. *Cancer Res.* **62,** 5189-5195.

(42) Meng, Q., Walker, D. M., McDonald, J. D., Henderson, R. F., Carter, M. M., Cook, D. L., Jr, McCash, C. L., Torres, S. M., Bauer, M. J., Seilkop, S. K., Upton, P. B., Georgieva, N. I., Boysen, G., Swenberg, J. A., and Walker, V. E. (2007) Age-, gender-, and species-dependent mutagenicity in T cells of mice and rats exposed by inhalation to 1,3-butadiene. *Chem. -Biol. Interact.* **166,** 121-131.

(43) Swenberg, J. A., Bordeerat, N. K., Boysen, G., Carro, S., Georgieva, N. I., Nakamura, J., Troutman, J. M., Upton, P. B., Albertini, R. J., Vacek, P. M., Walker, V. E., Sram, R. J., Goggin, M., and Tretyakova, N. (2010) 1,3-Butadiene: Biomarkers and application to risk assessment. *Chem. Biol. Interact.*

(44) Rusyn, I., Asakura, S., Li, Y., Kosyk, O., Koc, H., Nakamura, J., Upton, P. B., and Swenberg, J. A. (2005) Effects of ethylene oxide and ethylene inhalation on DNA adducts, apurinic/apyrimidinic sites and expression of base excision DNA repair genes in rat brain, spleen, and liver. *DNA Repair* **4,** 1099-1110.